Robust Optimization of Cognitive Radio Networks Powered by Energy Harvesting

Shimin Gong*, Lingjie Duan*, Ping Wang†
*Singapore University of Technology and Design
†Nanyang Technological University

***Abstract*—We consider a cognitive radio network, where primary users (PUs) share their spectrum with energy harvesting (EH) enabled secondary users (SUs), conditioned on a limited SUs' interference at PU receivers. Due to the lack of information exchange between SUs and PUs, the SU-PU interference channels are subject to uncertainty in channel estimation. Besides channel uncertainty, SUs' EH profile is also subject to spatial and temporal variations, which enforce an energy causality constraint on SUs' transmit power control and affect SUs' interference at PU receivers. Considering both the channel and EH uncertainties, we propose a robust design for SUs' power control to maximize SUs' throughput performance. Our robust design targets at the worst-case interference constraint to provide a robust protection for PUs, while guarantees a transmission probability to reflect SUs' minimum QoS requirements. To make the non-convex throughput maximization problem tractable, we develop a convex approximation for each robust constraint and successfully design a successive approximation approach that converges to the global optimum of the throughput objective. Simulations show that SUs will change transmission strategies according to PUs' sensitivity to interference, and we also exploit the impact of SUs' EH profile (e.g., mean, variance, and correlation) on SUs' power control.**

I. Introduction

Power control in underlay cognitive radio networks [1] relies on channel information between primary users (PUs) and secondary users (SUs). To harmoniously co-use PUs' licensed spectrum bands, SUs need to precisely estimate their channels to PU receivers such that their aggregate interference to PUs will not exceed a certain level. The aggregate interference at PU receivers is a joint effect of SUs' transmit power control and the SU-PU channel conditions, which can be obtained by SUs through overhearing PUs' ACK packets in a reciprocal channel [2]. However, such estimation is unreliable as PU receivers usually send back ACK packets sporadically after receiving a bulk of data streaming. Relying on out-of-date channel information easily leads to wrong estimation of the interference at PU receivers and violations of PUs' interference constraints.

To guarantee PUs' protection with channel uncertainty, some robust power control schemes are proposed to deal with channel variations in either a stochastic approach [3] or the worst-case robust approach [4]. A stochastic approach assumes that a channel gain follows a known distribution function, which leads to chance constraints in the power control problem. To make it analytically tractable, the chance constraints are further transformed into convex forms. For example, the channel gain is viewed as log-normal distributed in [3] and the distribution function of PUs' interference is approximately derived. In practice, however, this distribution information is often unavailable as the channel condition is time-varying in a short time scale and it is hard to collect enough data samples for immediate channel estimation. Alternately, the worst-case approach reasonably restricts the uncertain channel gain to be bounded in a convex uncertainty set, which does not require any prior knowledge about channel gain's distribution. For example, with a ball-shaped uncertainty set in [5], robust power control is proposed to minimize SUs' total power or maximize a weighted utility function, subject to interference constraints at PU receivers.

Prior works studying SUs' power control with channel uncertainty usually assume fixed energy supply (e.g., [1]–[5]). However, lacking the budget to afford spectrum license, SUs also want to reduce the energy cost or improve energy efficiency to meet their ever-increasing data traffic. Conventionally, SUs' devices are equipped with capacity-limited batteries which require periodic recharging or replacement to sustain network connectivity. In practice, the replacement of battery may be costly or the size of battery is too large for tiny wireless sensor nodes. To resolve the energy shortage, one approach is to minimize the energy consumptions in mobile device by optimal transmission scheduling [6] or offloading the computational tasks to cloud service [7]. Another approach relies on the recent development in energy harvesting (EH), which enables the mobile devices to obtain cheap energy from ambient environment (e.g, solar and wind energy) [8], [9]. However, the harvested energy is intermittent in nature and generally shows spatial and temporal variations. For example, the weather change (sunny, cloudy, or rainy) leads to time-varying EH rates and different geo-located mobile devices may have certain correlation in their EH profiles, e.g., nearby mobile devices may experience similar weather conditions and their harvested solar energy tend to change in a similar pattern.

Without full knowledge about the available energy, the power budget constraint is not determined thus causes new challenges for SUs' power control and performance maximization. If SUs' transmit power is greater than the EH rate, power outage happens which may cause packet loss

This work was supported by the SUTD-MIT International Design Centre (IDC) Grant (Project Number: IDSF1200106OH) and the SUTD-ZJU Joint Collaboration Grant (Project Number: ZJUR 041407). Lingjie Duan is the corresponding author.

978-1-4799-8381-0/15/$31.00 ©2015 IEEE

and require extra energy for retransmissions, degrading SUs' overall performance. The energy uncertainty in EH has been explicitly considered in [10] where robust beamforming is designed to maximize the worst-case harvested energy at a dedicated energy receiver. In this work, we jointly consider the uncertainties of channel information and energy profile in cognitive radio networks. By studying the interplay between these two uncertainties, we aim to design optimal power control scheme for SUs' throughput maximization. Our main contributions are summarized as follow:

- *Modeling Channel and EH Uncertainties*: Different from the stochastic or the worst-case robust model in literature (e.g., [3] and [4]), we consider a distribution uncertainty model, i.e., either channel gain or harvested energy is viewed as a random variable with an ambiguous distribution function subject to a uncertainty set. Specifically, we model the channel uncertainty using a probabilistic distance with respect to a known reference, while model energy uncertainty using its moment statistics.
- *Robust Energy and Interference Constraints*: Based on the uncertainty models, we define robust interference constraints to ensure robust protection for PUs by considering the worst-case estimation of channel gains from SU transmitters to PU receivers. To ensure desirable transmission opportunities for SUs, we define SUs' stochastic power budget constraints by setting an upper limit to their worst-case power outage probabilities.
- *Throughput Maximization with SUs' Power Control*: We formulate SUs' throughput maximization as a non-convex problem, subject to robust interference and energy constraints. We first propose convex approximations for the robust constraints and then employ successive approximation to solve the problem. By exploiting monotonicity in the problem, the proposed method yields the global optimal throughput performance.

The rest of this paper is organized as follows. We model SUs' EH and channel uncertainties in Section II, and define the robust energy and interference constraints in Section III. We formulate a non-convex throughput maximization problem in Section IV, and solve it by a successive approximation method. We show some numerical results in Section V and draw the conclusions in Section VI.

II. System Model

We consider a down-link cellular network consisting of K mobile devices as PUs spatially distributed under the coverage of a primary base station, which has fixed power supply. N mobile sensors as the SUs in an ad hoc network can access the same spectrum band of the primary network as long as they do not introduce intolerant interference to PUs. The sets of PUs and SUs are denoted by $\mathcal{K} = \{1, 2, \ldots, K\}$ and $\mathcal{N} = \{1, 2, \ldots, N\}$, respectively. We consider a practical scenario where there is no information exchange between SUs and PUs, but exists a common control channel [11] among SUs to communicate with each other. SUs can be either battery-free or battery-deployed depending on the cost to install batteries. Besides, each SU is capable of harvesting energy from ambient environment (e.g., solar, wind and vibration energy) and the energy harvester is able to simultaneously charge and discharge [8].

We consider a time-slotted model for SUs' EH and channel access. At each time slot $t \in \mathcal{T} \triangleq \{1, 2, \ldots, T\}$, SU $n \in \mathcal{N}$ decides its transmit power $p_n(t)$ at the beginning of time t by taking into account the available energy (and its statistical information) and the interference at PU receivers. Let $\varepsilon_n^s(t)$ denote the stored energy of SU n at the end of time slot t, thus $\varepsilon_n^s(t) = 0$ for battery-free SUs and $\varepsilon_n^s(t) \geq 0$ for battery-depolyed SUs. Let $\varepsilon_n^h(t)$ denote the harvested energy during time slot t, therefore, the total available energy for communication in time slot $t+1$ is $\varepsilon_n(t+1) = \varepsilon_n^s(t) + \varepsilon_n^h(t+1)$. According to the measurements in [12], outdoor solar energy is periodic and predictable in a time granularity of days. While the data transmission period is in the scale of milliseconds. Therefore, it is reasonable to assume that each SU's EH rate $\varepsilon_n^h(t)$ is constant over a time slot.

SUs' EH enforces an energy causality constraint on SUs' transmit power. Due to the spatial and temporal variations in EH, this power budget varies at different SUs and across time slots. In the following, we first present the uncertainty model for SUs' EH, and then describe the uncertainty model of channel gains between SU transmitters and PU receivers.

A. Energy Harvesting with Uncertainty

Due to the changing ambient environment and SUs' mobility over time slots, the EH rate in a time slot is random and an SU transmitter cannot predict the rate precisely. Thus, the SU is not sure about the total available energy at the beginning of each time slot. For simplicity, we denote $\boldsymbol{\varepsilon} = [\varepsilon_1, \varepsilon_2, \ldots, \varepsilon_N]$ as the total energy levels at individual SUs, which are random and follow a joint distribution function $f_{\boldsymbol{\varepsilon}}(\boldsymbol{x})$ with certain correlation structure. For example, when SUs are located nearby to harvest solar energy, they may experience similar weather conditions and their harvested energy tend to increase or decrease in a similar pattern. A fully understanding of SUs' correlation in EH will help to jointly design their transmit power to enhance SUs' performance and PUs' protection. However, the estimation of distribution $f_{\boldsymbol{\varepsilon}}(\boldsymbol{x})$ is computationally prohibitive and imprecise. Instead, industry prefers to measure the sample mean $\boldsymbol{\mu} = [\mu_1, \mu_2, \ldots, \mu_N]$ and the covariance matrix Σ as they are much easier to observe in practice and can be estimated with much higher accuracy. Given these moment information $(\boldsymbol{\mu}, \Sigma)$, we characterize the uncertain distribution uncertainty $f_{\boldsymbol{\varepsilon}}(\boldsymbol{x})$ by the following set:

$$\mathbb{U}_{f_{\boldsymbol{\varepsilon}}} = \left\{ f_{\boldsymbol{\varepsilon}}(\boldsymbol{x}) \;\middle|\; \begin{array}{l} \mathbb{E}_{f_{\boldsymbol{\varepsilon}}}\left[\mathbf{1}(\boldsymbol{\varepsilon} \in \mathcal{S})\right] = 1,\ \mathbb{E}_{f_{\boldsymbol{\varepsilon}}}\left[\boldsymbol{\varepsilon}\right] = \boldsymbol{\mu} \\ \mathbb{E}_{f_{\boldsymbol{\varepsilon}}}\left[(\boldsymbol{\varepsilon} - \boldsymbol{\mu})(\boldsymbol{\varepsilon} - \boldsymbol{\mu})^T\right] = \Sigma \end{array} \right\}, \quad (1)$$

where $\mathcal{S}$ dentes the set of all observations of $\boldsymbol{\varepsilon}$ and $\mathbf{1}(\cdot)$ is a indicator function. $\mathbb{U}_{f_{\boldsymbol{\varepsilon}}}$ defines a set of all possible distribution functions exhibiting the same statistical information (i.e., mean and variance) as we can extract from historical observations $\{\boldsymbol{\varepsilon}_t\}_{t \in \mathcal{T}}$. The actual distribution $f_{\boldsymbol{\varepsilon}}(\boldsymbol{x})$ may be in any shape and bear no closed-form expressions. It can be a mixture

of different well-known distributions with mean and variance equal to $\boldsymbol{\mu}$ and Σ, respectively. In a more practical case, the sample estimates $(\boldsymbol{\mu}, \Sigma)$ may be also uncertain and confined in a convex set [13]. However, adding this uncertainty will not affect our procedures in the analytical work. So we simply consider precise statistical information $(\boldsymbol{\mu}, \Sigma)$ in this paper.

B. Channel Estimation with Uncertainty

Precise estimation of channel condition is critical for SUs to measure the interference at PU receivers that guides the transmit power control at SU transmitters. Let h_{mn} denote the channel gain from SU transmitter $m \in \mathcal{N}$ to the SU receiver $n \in \mathcal{N}$. The estimation of h_{mn} can be accurate enough as it is assisted by the information exchange between the SU pair through the common control channel. However, the estimation of channel gain g_{nk} between SU transmitter $n \in \mathcal{N}$ and PU receiver $k \in \mathcal{K}$ is easily subject to estimation errors as PUs will not send feedback regularly to SUs. To model the uncertainty of g_{nk}, we consider g_{nk} as a random variable. Its distribution function $f_{nk}(x)$ is not exactly known but has limited difference to an empirical distribution $f^0_{nk}(x)$. Formally, the distribution uncertainty of g_{nk} is given as follows:

$$\mathbb{Z}_{nk} = \left\{ f_{nk}(x) \mid D_{KL}\left(f_{nk}(x), f^0_{nk}(x)\right) \le D_{nk} \right\}. \quad (2)$$

Here $f_{nk}(x)$ represents the actual distribution of channel gain through long term observations or precise estimation, while the known reference distribution $f^0_{nk}(x)$ is a closed-form empirical approximation. The distance measure from $f_{nk}(x)$ to its reference $f^0_{nk}(x)$ is defined in terms of Kullback-Leibler (KL) divergence [14], i.e., $D_{KL}\left(f_{nk}(x), f^0_{nk}(x)\right) = \mathbb{E}_{f_{nk}}\left[\ln f_{nk}(x) - \ln f^0_{nk}(x)\right]$, which should be less than a distance limit D_{nk}. In practice, we can set $f^0_{nk}(x)$ as a log-normal distribution and update it online according to the detection of new channel information as in [3].

III. Robust Energy and Interference Constraints

Given the energy and channel uncertainty models, we define probabilistic power budget constraints for SUs' and robust interference constraint for PUs' protection, respectively. For each constraint, we present convex transformation that simplifies SUs' throughput maximization problem.

A. Probabilistic Power Budget Constraint

Given the statistical information $(\boldsymbol{\mu}, \Sigma)$ and uncertainty set $\mathbb{U}_{f_{\boldsymbol{\varepsilon}}}$, each SU anticipates the energy fluctuations and optimizes its transmit power to improve the overall throughput in a time slot. In next time slot, the information $(\boldsymbol{\mu}, \Sigma)$ may change and the SU will adapt its transmit power to response to such changes. Due to limited response time, we assume that SUs use fixed transmit power $\boldsymbol{p}$ in each time slot. Thus, it is possible that an SU $n \in \mathcal{N}$ over-estimates the harvested energy ε^h_n in a time slot and sets the transmit power p_n higher than the instant value of ε_n. In this case, power outage happens and causes an interruption to SUs' data transmissions. Frequent transmission interruption results in resource wastage in both spectrum and energy. Therefore, we reasonably make a tradeoff by upper bounding the power outage probability:

$$\mathbb{E}_{f_{\boldsymbol{\varepsilon}}}[\mathbf{1}(p_n \ge \varepsilon_n)] \le \alpha. \quad (3)$$

Comparing to the information outage [15] that is defined in terms of unsuccessful reception of data, the power outage probability is a physical layer metric characterizing the transmission failure caused by insufficient energy supply, while information outage could be caused by multiple factors, e.g., channel fading, power outage, etc.

The quantification of SUs' power outage probability in LHS of (3) requires the knowledge of $f_{\boldsymbol{\varepsilon}}(x)$, which is uncertain and subject to a uncertainty set in (2). Therefore, we replace the probabilistic power budget constraint (3) by its worst-case counterpart

$$\min_{f_{\boldsymbol{\varepsilon}} \in \mathbb{U}_{\mathbb{P}}} \mathbb{E}_{f_{\boldsymbol{\varepsilon}}}[\mathbf{1}(p_n \le \varepsilon_n)] \ge 1 - \alpha, \quad (4)$$

Note that a chance constraint is generally non-convex and the uncertainty of $f_{\boldsymbol{\varepsilon}}(x)$ further complicates the quantification of power outage probability. To simplify this constraint, we first present a general convex approximation for the chance constraint in (3) and then find the robust counterpart in (4) by solving a convex moment problem.

Lemma 1: The chance constraint (3) can be approximated by a convex constraint as follows:

$$\min_{\beta} \alpha\beta + \mathbb{E}_{f_{\boldsymbol{\varepsilon}}}\left[(g_n(\boldsymbol{\varepsilon}) - \beta)^+\right] \le 0, \quad (5)$$

where $g_n(\boldsymbol{\varepsilon}) = p_n - \boldsymbol{e}_n^T\boldsymbol{\varepsilon}$ and $\boldsymbol{e}_n$ denotes the n-th column of the identity matrix.

The proof of Lemma 5 is similar to that in [16] and skipped here for conciseness. Without exact distribution information, the robust counterpart of (4) is simply given as

$$\min_{\beta \in \mathbb{R}} \alpha\beta + \max_{f_{\boldsymbol{\varepsilon}} \in \mathbb{U}_{\mathbb{P}}} \mathbb{E}_{f_{\boldsymbol{\varepsilon}}}\left[(g_n(\boldsymbol{\varepsilon}) - \beta)^+\right] \le 0. \quad (6)$$

The maximization operation ensures that the probabilistic power budget constraint (3) holds for any realization of distribution $f_{\boldsymbol{\varepsilon}}(x)$ in its uncertainty set $\mathbb{U}_{f_{\boldsymbol{\varepsilon}}}$. According to the definition of $\mathbb{U}_{f_{\boldsymbol{\varepsilon}}}$, the maximization operation in (6) involves the first and second moment statistics and we have the following proposition to further simplify this constraint.

Proposition 1: The worst-case probabilistic power budget constraint (6) is equivalent to a feasibility check as follows:

$$\exists \quad (\beta, \boldsymbol{\lambda}, Q, \kappa) \quad (7a)$$

$$s.t. \quad \alpha\beta + \kappa + \boldsymbol{\lambda}^T\boldsymbol{\mu} + Q \otimes \left(\Sigma + \boldsymbol{\mu}\boldsymbol{\mu}^T\right) \le 0 \quad (7b)$$

$$\begin{bmatrix} Q & \boldsymbol{\lambda}/2 \\ \boldsymbol{\lambda}^T/2 & \kappa \end{bmatrix} \succeq 0 \quad (7c)$$

$$\begin{bmatrix} Q & (\boldsymbol{\lambda} + \boldsymbol{e}_n)/2 \\ (\boldsymbol{\lambda} + \boldsymbol{e}_n)^T/2 & \kappa + \beta - p_n \end{bmatrix} \succeq 0, \quad (7d)$$

where κ, $\boldsymbol{\lambda}$, and Q are Lagrangian multipliers associated with the moment constraints in (1), respectively.

The proof of Proposition 1 is given in appendix A. Note that, the power outage probability constraint is defined for each

SU $n \in \mathcal{N}$, therefore the choice of β and dual variables $(\boldsymbol{\lambda}, Q, \kappa)$ are independent at each SUs. For fixed power outage level α, (7b) is a linear inequality and (7c), (7d) define two linear matrix inequalities. Therefore, the feasibility problem is efficiently tractable by convex optimization techniques.

B. Worst-Case Interference Constraint

Given this convex approximation of the probabilistic power budget constraint, SUs aim to maximize their throughput performance without introducing excessive interference to PUs. To guarantee PUs' protection under uncertain channel model (2), SUs need to estimate the worst-case interference at each PU $k \in \mathcal{K}$ and ensure it to be less than a pre-defined interference threshold ϕ_k:

$$\sum_{n=1}^{N} p_n g_{nk}^w \leq \phi_k, \quad \forall k \in \mathcal{K}, \tag{8}$$

where g_{nk}^w denotes the estimation of the worst-case channel gain. Note that, nominal channel gain g_{nk}^0 is simply the time average of all channel samples in a channel estimation period, while the worst-case channel gain g_{nk}^w is the largest estimation $\mathbb{E}_{f_{nk}}[g_{nk}]$ when distribution $f_{nk}(x)$ is subject to uncertainty set $\mathbb{Z}_{nk}$. Specifically, g_{nk}^w is given by following moment problem:

$$\max_{f_{nk}} \quad \mathbb{E}_{f_{nk}}\big[\, x \,\big] \tag{9a}$$

$$s.t. \quad \mathbb{E}_{f_{nk}}\big[\ln f_{nk}(x) - \ln f_{nk}^0(x)\big] \leq D_{nk} \tag{9b}$$

$$\mathbb{E}_{f_{nk}}\big[\mathbf{1}(x \in \mathcal{G})\big] = 1, \tag{9c}$$

where $\mathcal{G}$ denotes the set of all possible observations of channel gain g_{nk}. Constraint (9b) requires that the distribution of g_{nk} has a limited distance to the reference distribution $f_{nk}^0(x)$. Constraint (9c) is a normalization that enforces $f_{nk}(x)$ to be a probability distribution function. It is easy to verify that the moment problem (9a)-(9c) is convex thus we can achieve its optimum by using primal-dual decomposition. Given the dual variables $\nu > 0$ and τ associated with (9b) and (9c), respectively, we can obtain the worst-case channel gain distribution as follows:

$$f_{nk}^w(x) = f_{nk}^0(x) \frac{\exp\left(\frac{x}{\nu}\right)}{\exp\left(1 + \frac{\tau}{\nu}\right)}. \tag{10}$$

According to the normalization (9c), we have $\exp\left(1 + \frac{\tau}{\nu}\right) = \Sigma(\nu) \triangleq \int f_{nk}^0(x) \exp\left(\frac{x}{\nu}\right) dx$. Therefore, we can set $\tau = \nu\left(\log \Sigma(\nu) - 1\right)$ and the worst-case distribution $f_{nk}^w(x|\nu)$ is merely parameterized by ν. By the KKT conditions:

$$D_{KL}\left(f_{nk}^w, f_{nk}^0 \,|\, \nu\right) - D_{nk} = 0, \tag{11}$$

we can pinpoint the solution ν^* as well as the worst-case distribution $f_{nk}^w(x|\nu^*)$. Though a direct solution to (11) is not possible, Lemma 1 in [17] ensures that the parameterized $D_{KL}\left(f_{nk}^w, f_{nk}^0 \,|\, \nu\right)$ is monotonically decreasing with respect to ν, which motivates a bisection method to search for ν^*.

IV. SUs' Robust Power Control

Setting a small power outage probability α restricts SUs to have low transmit power. It thus reduces the interruptions to SUs' transmissions but also brings down SUs' data rate. In another aspect, setting higher power outage probability permits SUs to transmit more aggressively with higher transmit power. It may achieve high instantaneous data rate if the transmission is successful, but SUs' total throughput is not necessarily increased as SUs face frequent transmission interruptions. Therefore, SUs' power control has to carefully choose a power outage probability $\alpha_n \in [\alpha_{min}, \alpha_{max}]$ for each SU $n \in \mathcal{N}$, then we can define SU's effective throughput as $r_n = (1 - \alpha_n)\log\big(1 + \gamma_n\big)$, where γ_n is the SINR at SU receiver n and given by $\gamma_n = \frac{p_n h_{nn}}{\sigma_n^2 + \pi_n + \sum_{m \neq n} p_m h_{mn}}$ where σ_n^2 is the noise density and π_n is the interferences from PUs. Our objective is to maximize SUs' sum throughput by jointly optimizing SU's transmit power p_n and power outage probability α_n, subject to SUs' power budget (7b)-(7d) and PUs' interference constraints (8):

$$\max_{\boldsymbol{\alpha}, \boldsymbol{p}, W} \quad \sum_{n \in \mathcal{N}} (1 - \alpha_n) \log\big(1 + \gamma_n(\boldsymbol{p})\big) \tag{12a}$$

$$s.t. \quad \sum_{n=1}^{N} p_n g_{nk}^w \leq \phi_k, \tag{12b}$$

$$\alpha_n \beta_n + \kappa_n + \boldsymbol{\lambda}_n^T \boldsymbol{\mu} + Q_n \otimes \big(\Sigma + \boldsymbol{\mu}\boldsymbol{\mu}^T\big) \leq 0, \tag{12c}$$

$$\begin{bmatrix} Q_n & \boldsymbol{\lambda}_n/2 \\ \boldsymbol{\lambda}_n^T/2 & \kappa_n \end{bmatrix} \succeq 0, \tag{12d}$$

$$\begin{bmatrix} Q_n & (\boldsymbol{\lambda}_n + \boldsymbol{e}_n)/2 \\ (\boldsymbol{\lambda}_n + \boldsymbol{e}_n)^T/2 & \kappa_n + \beta_n - p_n \end{bmatrix} \succeq 0, \tag{12e}$$

$$\forall\, k \in \mathcal{K} \text{ and } n \in \mathcal{N}, \tag{12f}$$

where $W = [\boldsymbol{\omega}_1, \ldots, \boldsymbol{\omega}_N]$ is a matrix with each column denoting independent choices of dual variables $\boldsymbol{\omega}_n = (\beta_n, \boldsymbol{\lambda}_n, Q_n, \kappa_n)$[1]. Note that convex approximation (12c)-(12e) implicitly gives an upper bound for SUs' transmit power. The PUs' interference power constraint (12b) also introduces a power budget which is coupled at different SUs. Therefore, SUs' power control has to coordinate between channel and energy uncertainties to maximize SUs' sum throughput.

A direct solution to (12a)-(12f) is difficult as the object (12a) is not concave and (12c) is non-convex. To shed some insight on the algorithm design, we first consider a simple case with only one SU. Let $\bar{\alpha}_n = 1 - \alpha_n$ denote the transmission probability and remove the subscripts n, problem (12a)-(12f)

[1]The variables $\beta_n, \kappa_n, \boldsymbol{\lambda}_n, Q_n$ may be of different size. We rearrange each element of the dual variables in a vector $\boldsymbol{\omega}_n$ for ease of presentation.

is degenerated into the following form:

$$\max_{\bar{\alpha},\gamma,\boldsymbol{\omega}} \quad \bar{\alpha}\log(1+\gamma) \tag{13a}$$

$$s.t. \quad \gamma g_k^w \le h\phi_k, \quad \forall\, k \in \mathcal{K}, \tag{13b}$$

$$(1-\bar{\alpha})\beta + \kappa + \lambda\mu + Q(\Sigma+\mu^2) \le 0, \tag{13c}$$

$$\begin{bmatrix} Q & \lambda/2 \\ \lambda/2 & \kappa \end{bmatrix} \succeq 0, \tag{13d}$$

$$\begin{bmatrix} Q & (\lambda+1)/2 \\ (\lambda+1)/2 & \kappa+\beta-\gamma/h \end{bmatrix} \succeq 0, \tag{13e}$$

For a single SU, we simply denote $\gamma = hp$ where p is SU's transmit power and $h = \frac{h_{nn}}{\sigma^2+\pi}$ denotes the channel gain between SU's transceiver normalized by the noise and the interference from PUs. Now we can see that the objective function $r(\bar{\alpha},\gamma)$ in (13a) is strictly increasing with respect to the transmission probability $\bar{\alpha}$ and SU's SINR γ. The monotonicity of $r(\bar{\alpha},\gamma)$ implies that the maximum of (13a) will be achieved on a boundary point of its feasible set Ω, denoted in a compact form as

$$\Omega = \{(\bar{\alpha},\gamma) \,|\, \exists\, \boldsymbol{\omega} \text{ s.t. } (13b)-(13e) \text{ hold with } (\bar{\alpha},\gamma)\}. \tag{14}$$

This property motivates the development of monotonic optimization method [18], which will be tailored in this paper to maximize SUs' sum throughput in a distributed way. To locate the optimal solution $(\bar{\alpha}^*,\gamma^*) \in \Omega$, we identify some properties of Ω that will be useful in the following discussions.

Definition 1: A set Ω is *normal* if $\boldsymbol{z}' \in \Omega$ for all $0 \preceq \boldsymbol{z}' \preceq \boldsymbol{z}$ and $\boldsymbol{z} \in \Omega$. A point $\boldsymbol{z} \in \Omega$ is an *upper boundary point* if $\boldsymbol{z}' \notin \Omega$ for all $\boldsymbol{z}' \succeq \boldsymbol{z}$ and $\boldsymbol{z}' \neq \boldsymbol{z}$. The set of upper boundary point is called the *upper boundary* of Ω, denoted by $\overline{\Omega}$.

Lemma 2: The feasible region Ω in (14) is normal and the optimum of (13a)-(13e) is achieved on $\overline{\Omega}$.

The proof of Lemma 2 is given in Appendix B. The basic idea of monotonic optimization is to successively approximate the feasible set Ω by generating a sequence of *regular-shaped* normal sets (i.e., polyblocks) P_l such that $P_0 \supset P_1 \supset \cdots \supset P_l \supset \cdots \supset \Omega$, by starting from an initial polyblock P_0. The construction of polyblock P_l is to approximate Ω by a *finite set* of boxes in the form of $[\mathbf{0},\boldsymbol{v}]$ where $\boldsymbol{v}$ is the vertex of a box set, as illustrated in Fig. 1. In each iteration l, the algorithm determines an upper bound r_l^U of the global optimum $r^* \triangleq \max_{\boldsymbol{z}\in\Omega} r(\boldsymbol{z})$ on the vertices of P_l and updates a lower bound r_l^L by evaluating the objective function on an upper boundary point of Ω. The algorithm terminates until the upper and lower bounds converge to the same within an acceptable error distance.

A. Update Lower and Upper Bounds

Let V_l denote the vertex set of polyblock P_l. The upper bound r_l^U can be easily determined on the vertices $\boldsymbol{v} \in V_l$ according to the monotonicity of $r(\bar{\alpha},\gamma)$. Let $\boldsymbol{z}_l = \arg\max_{\boldsymbol{v}\in V_l} r(\boldsymbol{v})$, then $r_l^U = r(\boldsymbol{z}_l)$ is an upper bound of the optimal throughput r^*. To determine a lower bound of r^*, we geometrically project $\boldsymbol{z}_l$ onto the upper boundary $\overline{\Omega}$ as illustrated in Fig. 1. The projection point $\boldsymbol{o}_l$ is the intersection

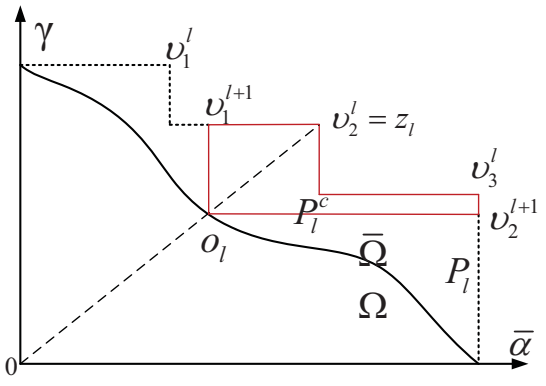

Fig. 1: Polyblock approximation.

between the upper boundary $\overline{\Omega}$ and a straight line from $\boldsymbol{z}_l$ to a reference point, normally, the origin $\mathbf{0}$ [18]. Then we can evaluate the lower bound as $r_l^L = r(\boldsymbol{o}_l)$. Note that $\boldsymbol{o}_l$ is a scaled version of $\boldsymbol{z}_l$. Let $\boldsymbol{o}_l = s_l\boldsymbol{z}_l$ and the scaling factor $s_l \in [0,1]$ is obtained by the projection problem as follows:

$$s_l = \max_s \{s \,|\, s\boldsymbol{z}_l \in \Omega\}. \tag{15}$$

That is, we need to find the maximum scaling factor s_l such that $\boldsymbol{o}_l(s_l) \triangleq s_l\boldsymbol{z}_l \in \overline{\Omega}$. Since Ω is a normal set, it is easy to verify that $\boldsymbol{o}_l(s) \notin \Omega$ for any $s_l < s \le 1$ and $\boldsymbol{o}_l(s) \in \Omega$ for any $0 \le s \le s_l$, which suggests a bisection method to pinpoint the value of s_l.

In each iteration of the bisection method, checking $\boldsymbol{o}_l(s) \in \Omega$ with fixed s is equivalent to check the feasibility of (13b)-(13e) with the variable $(\bar{\alpha},\gamma)$ replaced by fixed point $(s\bar{\alpha}_l, s\gamma_l)$. Thus, inequality (13b) becomes linear and convex with respect to $\boldsymbol{\omega} = (\beta,\kappa,\lambda,Q)$. Therefore, this formulation is efficiently tractable by interior-point method. Once we determine the projection $\boldsymbol{o}_l$, we evaluate the function value $r(\boldsymbol{o}_l)$ which is achievable in set Ω and thus can serve as a tighter lower bound r_l^L of r^* if $r(\boldsymbol{o}_l) \ge r_{l-1}^L$.

B. Generation of New Polyblock

If $\boldsymbol{z}_l = \arg\max_{\boldsymbol{v}\in V_l} r(\boldsymbol{v})$ happens to be on the upper boundary $\overline{\Omega}$ (i.e., $\boldsymbol{z}_l$ coincides with its projection $\boldsymbol{o}_l \in \overline{\Omega}$ with $s_l = 1$), then $r_l^U = r_l^L$ and $\boldsymbol{z}_l$ is the global optimal solution. Otherwise we will generate a "smaller" polyblock $P_{l+1} \subset P_l$ by updating the vertex set V_{l+1} to find either a tighter upper or lower bound of r^*. Now assuming $\boldsymbol{z}_l \notin \overline{\Omega}$ as shown in Fig. 1, we have $\Omega \bigcap P_l^c = \emptyset$ where $P_l^c \triangleq \{\boldsymbol{z} \in P_l \,|\, \boldsymbol{z} \succeq \boldsymbol{o}_l\}$ denotes the red hexagon in Fig. 1. Since Ω is a normal set, removing this P_l^c from polyblock P_l will not affect the optimum of $r(\bar{\alpha},\gamma)$ in its feasible set Ω. Moreover, the removal of P_l^c will generate new vertices and erase some redundant vertices in V_l.

Let $\overline{V}_l(\boldsymbol{o}_l) = \{\boldsymbol{v} \in V_l \,|\, \boldsymbol{v} \succeq \boldsymbol{o}_l\}$ denote the vertices of box set P_l^c. For example, we have $\overline{V}_l(\boldsymbol{o}_l) = \{\boldsymbol{v}_2^l = \boldsymbol{z}_l, \boldsymbol{v}_3^l\}$ as shown in Fig. 1. Note that $\overline{V}_l$ is non-empty and contains at least $\boldsymbol{z}_l$. We further define the reflection of $\boldsymbol{o}_l$ as $\bar{\boldsymbol{z}}_l$ such that $\bar{\boldsymbol{z}}_l(i) = \max_{\boldsymbol{v}\in\overline{V}_l(\boldsymbol{o}_l)} \boldsymbol{v}(i)$ for $1 \le i \le \dim(\boldsymbol{o}_l)$[2],

[2]$\dim(\boldsymbol{o}_l)$ denotes the dimension of $\boldsymbol{o}_l$ and here we have $\dim(\boldsymbol{o}_l) = 2$.

where $\boldsymbol{v}(i)$ and $\bar{\boldsymbol{z}}_l(i)$ denote the i-th entry in vectors $\boldsymbol{v}$ and $\bar{\boldsymbol{z}}_l$, respectively. Then we can find the new vertices $\boldsymbol{v}_i^{l+1} = \boldsymbol{o}_l + \Lambda_i(\bar{\boldsymbol{z}}_l - \boldsymbol{o}_l)$, for $1 \le i \le \dim(\boldsymbol{o}_l)$. Here Λ_i is a zero matrix with the i-th diagonal element set to 1. The new vertex set V_{l+1} will include all newly generated vertices $\boldsymbol{v}_i^{l+1}$ and exclude all redundant vertices in set $\overline{V}_l$. With a little abuse of notation, it is updated as follows:

$$V_{l+1} = V_l - \overline{V}_l + \{\boldsymbol{v}_i^{l+1}\}_{0 \le i \le \dim(\boldsymbol{o}_l)}. \tag{16}$$

Once we update set V_{l+1}, we can construct polyblock P_{l+1} as the union of finite boxes, i.e., $P_{l+1} = \bigcup_{\boldsymbol{v} \in V_{l+1}} [0, \boldsymbol{v}]$.

Algorithm 1 Successive Polyblock Approximation

1: set initial polyblock P_l, $r_l^U = 1$, and $r_l^L = 0$ for $l = 0$
2: while $|r_l^U - r_l^L| \ge \epsilon$
3: $\quad l \leftarrow l + 1$
4: $\quad$ update $\boldsymbol{z}_l = \arg\max_{\boldsymbol{v} \in V_{l-1}} r(\boldsymbol{v})$ and $r_l^U = r(\boldsymbol{z_l})$
5: $\quad$ if $\boldsymbol{z}_l \in \Omega$ then
6: $\quad\quad$ update $r_l^L = r(\boldsymbol{z}_l)$
7: $\quad$ else
8: $\quad\quad$ find projection $\boldsymbol{o}_l = s_l \boldsymbol{z}_l \in \overline{\Omega}$
9: $\quad\quad$ update $r_l^L = r(\boldsymbol{o}_l)$ if $r(\boldsymbol{o}_l) \ge r_l^L$
10: $\quad\quad$ update vertex set V_l by (16)
11: $\quad$ end if
12: end while
13: set $\boldsymbol{z}^* = \boldsymbol{z}_l$ and $r^* = r(\boldsymbol{z}^*)$

The detailed steps are organized in Algorithm 1. To initialize the polyblock P_0, we can simply set $\bar{\alpha} = 1$ and λ to its maximum value. Then Algorithm 1 continues to update an upper bound (in line 4 of Algorithm 1) and a lower bound (in line 5-11 of Algorithm 1) of the optimal objective until a tolerance level ϵ ensuring an ϵ-optimal solution $(\bar{\alpha}^*, \gamma^*)$. As shown in [18], Algorithm 1 is guaranteed to converge to an ϵ-optimal solution after finite number of iterations for any $\epsilon > 0$. Fig. 2 shows an illustrative example of Algorithm 1. For fixed transmission probability $\bar{\alpha}$, problem (13a)-(13e) becomes convex and we can find the maximum SINR γ efficiently. All these numerically calculated points $(\bar{\alpha}, \gamma)$ form the upper boundary $\overline{\Omega}$, which is denoted by the dashed line in Fig. 2(a). Observing the shape of curve $\overline{\Omega}$, the feasible region Ω is normal and the successive approximation method works well. When the generation of polyblocks, denoted by the solid lines in Fig. 2(a), becomes closer to the global optimum, denoted by "*" marker, the gap between r_l^U and r_l^L is diminishing to the desired accuracy as shown in Fig. 2(b).

C. Distributed Power Control in multi-SUs Case

Our previous discussion is regarding a single SU, but the successive polyblock approximation can be easily extended to multiple SUs. Let $\boldsymbol{z}_n = (\bar{\alpha}_n, \gamma_n)$ denote the strategy of SU n and $Z = \{\boldsymbol{z}_n\}_{n \in \mathcal{N}} \triangleq (\bar{\boldsymbol{\alpha}}, \boldsymbol{\gamma})$ be the strategy of N SUs. Though there is a significant increase in problem dimensions, the projection problem (15) and the vertex update (16) can be derived in a similar procedure. Moreover, we observe that

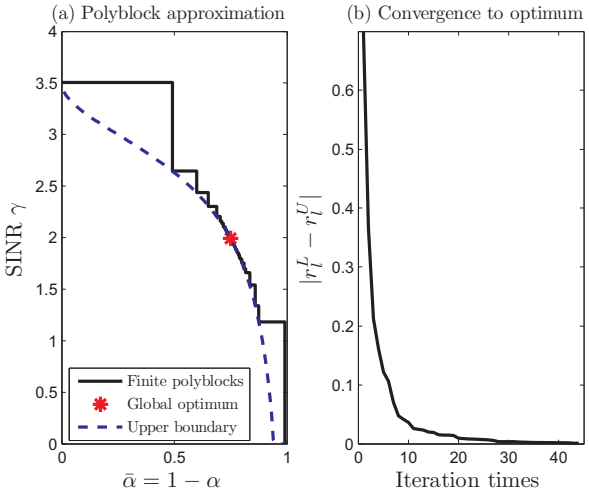

Fig. 2: An illustrative example.

different SU's strategy $\boldsymbol{z}_n$ is only coupled with each other through the interference constraint (12b). Taking apart this coupled constraint, we can decompose the projection problem (15) into N subproblems at individual SUs. As such, we rewrite the feasible region of (12a)-(12f) as

$$\Omega^N = \{Z \,|\, \boldsymbol{z}_n = (\bar{\alpha}_n, \gamma_n) \in \Omega_n, \forall n \in \mathcal{N}, \text{ and } G_w \boldsymbol{p} \le \boldsymbol{\phi}\},$$

where Ω_n is defined in (14) for each SU $n \in \mathcal{N}$ and $G_w \boldsymbol{p} \le \boldsymbol{\phi}$ is a compact form of the interference constraints in (12b). The matrix coefficient G_w represents the worst-case channel gain from SU transmitter to PU receiver, that is determined by solving the moment problem (9a)-(9c).

To apply Algorithm 1, we have to check the feasibility of a strategy profile $(\bar{\boldsymbol{\alpha}}, \boldsymbol{\gamma})$ and project it onto the upper boundary of Ω^N if $(\bar{\boldsymbol{\alpha}}, \boldsymbol{\gamma}) \notin \Omega^N$. Firstly, a feasible SINR profile $\boldsymbol{\gamma}$ has to satisfy the interference constraint $G_w \boldsymbol{p} \le \boldsymbol{\phi}$. Note that, SUs' SINR profile $\boldsymbol{\gamma}$ relates to SUs' transmit power vector $\boldsymbol{p}$ through $\big(\mathbf{1} - \overline{H}(\boldsymbol{\gamma})\big)\boldsymbol{p} = \boldsymbol{\eta}(\boldsymbol{\gamma})$ with

$$\big[\overline{H}(\boldsymbol{\gamma})\big]_{nm} = \begin{cases} 0, & m = n \\ \gamma_n \frac{h_{nm}}{h_{nn}}, & m \ne n \end{cases}$$

and $[\boldsymbol{\eta}(\boldsymbol{\gamma})]_n = \gamma_n \frac{\sigma_n^2 + \pi_n}{h_{nn}}$. Thus the interference constraint $G_w \boldsymbol{p} \le \boldsymbol{\phi}$ can be rewritten as follows:

$$\mathbf{0} \le \overline{G}_w \big(1 - \overline{H}(\boldsymbol{\gamma})\big)^{-1} \boldsymbol{\eta}(\boldsymbol{\gamma}) \le \mathbf{1}, \tag{17}$$

where $\mathbf{0}$ and $\mathbf{1}$ are all-zero and all-one vectors with proper size, respectively. $[\overline{G}_w]_{nm} = [G_w]_{nm}/\phi_n$ denotes the worst-case channel matrix normalized by PUs' interference threshold $\boldsymbol{\phi}$. If the interference constraint (17) holds with the SINR profile $\boldsymbol{\gamma}$, we thus discard $G_w \boldsymbol{p} \le \boldsymbol{\phi}$ from the feasible set Ω^N. Then we continue to check whether $\boldsymbol{z}_n = (\bar{\alpha}_n, \gamma_n)$ is feasible in Ω_n for all $n \in \mathcal{N}$, which can be performed independently at individual SUs. If $\boldsymbol{z}_n$ is feasible for all $n \in \mathcal{N}$, the optimum is achieved with $Z = (\bar{\boldsymbol{\alpha}}, \boldsymbol{\gamma})$, otherwise, we need to scale down Z and project it onto the upper boundary of Ω^N. Let

$Z^l = (\bar{\boldsymbol{\alpha}}^l, \boldsymbol{\gamma}^l) \notin \Omega^N$ be the optimal vertex at iteration l, the projection of Z^l is to find a scaling factor s_l such that

$$s_l = \max_s \left\{ s : (s\bar{\alpha}_n^l, s\gamma_n^l) \in \Omega_n, \forall\, n \in \mathcal{N} \right\},$$

which can be solved by a bisection method independently at individual SUs.

V. Numerical Results

In this section, without loss of generality, we consider $N = 3$ SU transceiver pairs and $K = 1$ PU receiver. We can easily extend to more SUs and PUs at the cost of a linear increase in the computational complexity. We set noise level n_0 as -100dBm and PU's interference power threshold ϕ as -35dBm. PUs' interference π_n at each SU receiver is viewed as constant and can be estimated by individual SUs before data transmissions. The mean path loss is an exponential function of the distance between transceivers with the path-loss exponent given by 3.5. In each simulation, we randomly generate locations for different users and estimate the channel matrix $H = [h_{nm}]_{n,m\in\mathcal{N}}$ and $G = [g_{nk}]_{n\in\mathcal{N},k\in\mathcal{K}}$, respectively. The estimation of channel gain h_{nm} between any two SUs is precise but the estimation of g_{nk} from SU transmitter n to PU receiver k is subject to a distribution uncertainty due to the lack of communications between SUs and PUs. To define the channel uncertainty in (2), we assume a Gaussian reference distribution and set the distance limit as $D_{nk} = 0.03$ [19]. The available energy $\boldsymbol{\varepsilon}$ at individual SUs is a random vector, with only mean and variance information available. To investigate how SUs' performance changes when SUs have different energy profiles, we gradually increase SUs' EH rates by setting different mean values of the harvested energy as $\boldsymbol{\mu}_1 = [4, 5, 6]$, $\boldsymbol{\mu}_2 = [5, 6, 7]$, and $\boldsymbol{\mu}_3 = [6, 7, 8]$, respectively.

Fig. 3(a) plots the comparison of SUs' sum throughput with three different mean values. We also show the throughput of individual SUs in Fig. 3(b) for the cases with $\boldsymbol{\mu}_1$ and $\boldsymbol{\mu}_3$ for a clear comparison. In both figures, we observe that SUs have a better throughput performance when the mean harvested energy levels are increased at individual SUs. The increase of SUs' energy level relaxes the power budget and allows SUs to transmit with higher power. But the potential for throughput improvement differs with PUs' interference threshold ϕ. Note from problem (12a)-(12f), both the interference threshold ϕ and the power outage probability threshold α enforce implicit upper bounds on SUs' transmit power. Thus, the actual throughput performance is a balance between these two aspects. When interference threshold is small, i.e., $\phi \leq -40$dBm, PUs have stringent interference requirements and it is more critical for SUs to control the interference power at PU receivers. In this case, the interference constraint becomes active, and it's not possible for SUs to significantly improve throughput performance even with sufficient energy supply. When PUs' interference constraint is relaxed (i.e., ϕ increases from -40dB to -35dBm), the potential of throughput improvement can be fully explored by increasing SUs' transmit power as shown in Fig. 4, where we plot SUs' optimal

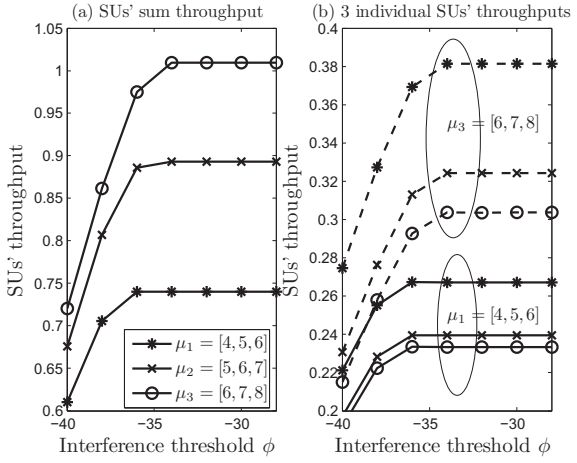

Fig. 3: Throughput increases with larger EH rates.

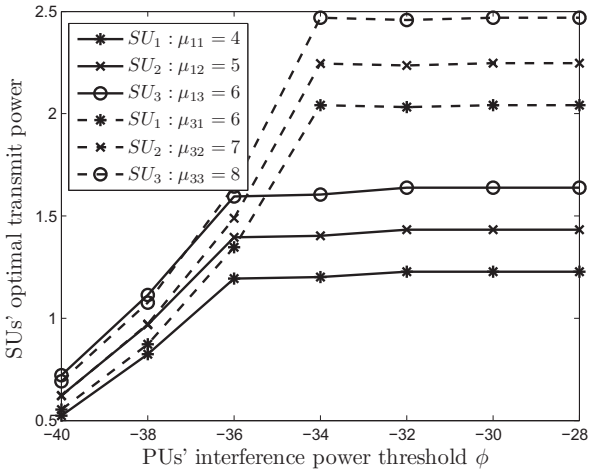

Fig. 4: SUs' transmit power updates according to ϕ.

transmit power under different interference threshold (legend μ_{in} denotes the mean energy level of SU n within the setting $\boldsymbol{\mu}_i$). However, when ϕ is further increased, the power outage probability constraint becomes active. Thus, SUs' transmit power achieves the maximum level as shown in Fig. 4.

In Fig. 5, we plot SUs' power outage probability and PUs' normalized interference power (i.e., perceived interference power normalized by PU's interference threshold ϕ) with different interference thresholds ϕ. Firstly, we observe that, for a fixed interference threshold, a higher EH rate allows SUs to transmit with potentially larger power and results in higher interference at PU receivers as shown in Fig. 5(a). However, the increase of transmit power does not necessarily introduce high power outage probability at SUs. Simulation shows that SUs' power outage probability can decrease with the increase of harvested energy as shown in Fig. 5(b). This is because, along the increase of SUs' transmit power, SUs also introduce stronger interference to each other, which reduces SUs' throughput performance. Thus, the optimal power

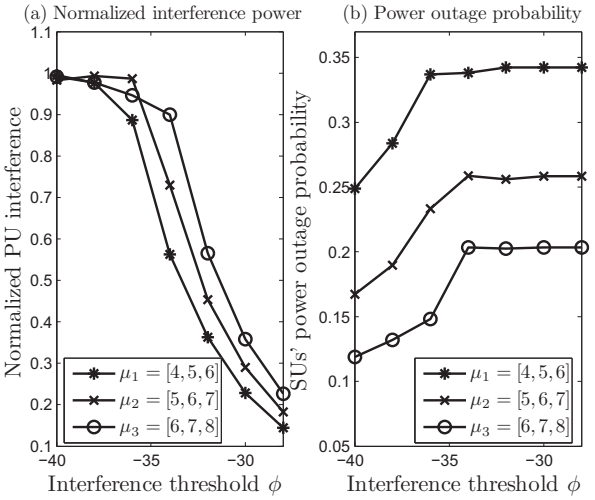

Fig. 5: The balance between interference and power outage.

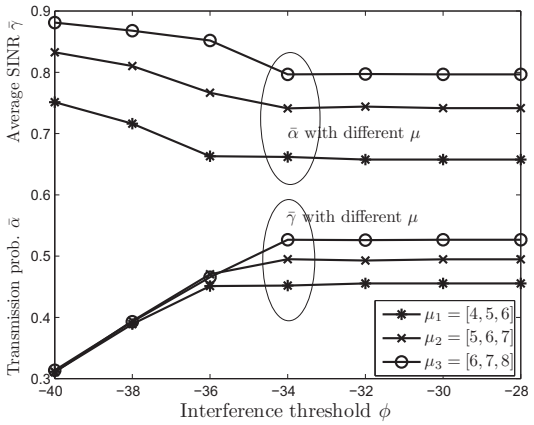

Fig. 6: SUs' optimal transmission probability and SINR.

control strategy will prevent SU to increase its transmit power proportionally to the increase of harvested energy.

Secondly, for fixed EH profile, we observe gradual increase of SUs' transmit power in Fig. 4 and power outage probability in Fig. 5(b) when PUs relax the interference threshold ϕ. We may conclude that, to maximize SUs' weighted sum throughput, SUs will optimize a smaller power outage probability when PUs are more sensitive to SUs' interference. In this case, PUs' stringent interference constraints prevent SUs to increase their data rate by transmitting at larger power. So SUs' throughput maximization mainly relies on the increase of transmission probability, i.e., with less interruptions in data transmissions, SUs can maintain a relatively fluent data flow to maximize the overall throughput even with low transmit power. On the contrary, SUs prefer setting an aggressively larger power outage probability when PUs are tolerable to higher interference. In this case, SUs can achieve high instantaneous throughput in one successful transmission, though SUs' transmission are frequently interrupted. This result is further verified by the observations in Fig. 6, where we show $(\bar{\alpha}, \bar{\gamma})$ for different values of $\boldsymbol{\mu}$. Here $\bar{\gamma}$ is SUs' average SINR. We see that, SUs' throughput increment mainly attributes to the increase of transmission probability at small ϕ while attribute to the increase of SUs' data rate at large ϕ.

VI. Conclusions

In this paper, we design a robust power control algorithm to maximize SUs' sum throughput with indeterministic power budget constraint due to the stochastic nature in energy harvesting. To protect PUs from excessive interference, SUs' power control is also challenged by the uncertain channel information from SU transmitters to PU receivers. We define probabilistic power budget constraint to account for the random variations in SUs' energy supply and rely on the worst-case channel estimation to ensure robust PU protection. To maximum SUs' sum throughput, the power control algorithm has to tradeoff between the uncertainties in EH and channel estimation. Simulation results show that, when PUs' interference threshold ϕ is low, SUs prefer to increase their transmission probability by transmitting at a low data rate. When PUs' interference threshold ϕ is high, SUs switch to a more aggressive strategy that accumulates their throughput in only few successful transmissions.

Appendix

A. Proof of Proposition 1

Proof: The minimum over $\beta \in \mathbb{R}$ in (6) implies that, this constraint will hold true if there exists some β such that

$$\beta + \frac{1}{\alpha} \max_{f_{\boldsymbol{\varepsilon}} \in \mathbb{U}_{f_{\boldsymbol{\varepsilon}}}} \mathbb{E}_{f_{\boldsymbol{\varepsilon}}} \big[(g(\boldsymbol{\varepsilon}) - \beta)^+ \big] \leq 0, \tag{18}$$

while the second term of (18) requires the solution to the following moment problem:

$$\max_{f_{\boldsymbol{\varepsilon}}} \quad \mathbb{E}_{f_{\boldsymbol{\varepsilon}}} \big[(g(\boldsymbol{\varepsilon}) - \beta)^+ \big] \tag{19a}$$

$$s.t. \quad \mathbb{E}_{f_{\boldsymbol{\varepsilon}}} \big[\mathbf{1}(\boldsymbol{\varepsilon} \in \mathcal{S}) \big] = 1, \tag{19b}$$

$$\mathbb{E}_{f_{\boldsymbol{\varepsilon}}} \big[\boldsymbol{\varepsilon} \big] = \boldsymbol{\mu}, \tag{19c}$$

$$\mathbb{E}_{f_{\boldsymbol{\varepsilon}}} \big[(\boldsymbol{\varepsilon} - \boldsymbol{\mu}) (\boldsymbol{\varepsilon} - \boldsymbol{\mu})^T \big] = \Sigma. \tag{19d}$$

The last two constraints require the mean and covariance of any distribution $f_{\boldsymbol{\varepsilon}}(\boldsymbol{x}) \in \mathbb{U}_{f_{\boldsymbol{\varepsilon}}}$ to be consistent with the measured mean and covariance, respectively. Constraint (19b) is a normalization which enforces $f_{\boldsymbol{\varepsilon}}(\boldsymbol{x})$ to be a probability distribution. Introducing dual variables $\kappa \in \mathbb{R}$, $\boldsymbol{\lambda} \in \mathbb{R}^N$, and positive semi-definite matrix $Q \in \mathbb{S}_+^N$ to constraints (19b)-(19d), respectively, the Lagrange function is given as

$$\begin{aligned} \Gamma(f_{\boldsymbol{\varepsilon}}, \kappa, \boldsymbol{\lambda}, Q) \;=\; & \kappa + \boldsymbol{\lambda}^T \boldsymbol{\mu} + Q \otimes (\Sigma + \boldsymbol{\mu}\boldsymbol{\mu}^T) \\ & + \mathbb{E}_{f_{\boldsymbol{\varepsilon}}} \big[(g(\boldsymbol{\varepsilon}) - \beta)^+ - \kappa - \boldsymbol{\lambda}^T \boldsymbol{\varepsilon} - \boldsymbol{\varepsilon}^T Q \boldsymbol{\varepsilon} \big], \end{aligned}$$

where $\otimes$ denotes the Frobenius product of two matrices, i.e., $A \otimes B = \mathbf{Tr}(AB^T)$. Then we get its dual problem as follows:

$$\min_{\boldsymbol{\lambda}, Q, r} \quad \kappa + \boldsymbol{\lambda}^T \boldsymbol{\mu} + Q \otimes \left(\Sigma + \boldsymbol{\mu}\boldsymbol{\mu}^T \right) \tag{20a}$$

$$s.t. \quad \boldsymbol{\varepsilon}^T Q \boldsymbol{\varepsilon} + \boldsymbol{\lambda}^T \boldsymbol{\varepsilon} + \kappa \geq 0, \quad \forall \boldsymbol{\varepsilon} \in \mathbb{R}^N, \tag{20b}$$

$$\boldsymbol{\varepsilon}^T Q \boldsymbol{\varepsilon} + \boldsymbol{\lambda}^T \boldsymbol{\varepsilon} + \kappa \geq g(\boldsymbol{\varepsilon}) - \beta, \quad \forall \boldsymbol{\varepsilon} \in \mathbb{R}^N. \tag{20c}$$

The feasibility and convexity of problem (19a)-(19d) ensures that strong duality holds and therefore the dual problem (20a)-(20c) will achieve the same worst-case probability as in (19a).

Note that the quadratic polynomial in LHS of (20b) is always non-negative when $\boldsymbol{\varepsilon}$ takes any realization in its feasible set $\mathcal{S}$. We can transform it into a linear matrix inequality:

$$\begin{bmatrix} Q & \boldsymbol{\lambda}/2 \\ \boldsymbol{\lambda}^T/2 & \kappa \end{bmatrix} \succeq 0.$$

A similar transformation can be applied to (20c). Therefore, we fairly obtain the equivalence in (7a)-(7d) by integrating (20a)-(20c) with constraint (18). ■

B. Proof of Lemma 2

Proof: To proof this lemma, we need to show that, for any $(\bar{\alpha}_1, \gamma_1) \succeq (\bar{\alpha}_2, \gamma_2) \succeq 0$, we have $(\bar{\alpha}_2, \gamma_2) \in \Omega$ if $(\bar{\alpha}_1, \gamma_1) \in \Omega$. Assume $\boldsymbol{\omega}_i = (\beta_i, \lambda_i, Q_i, \kappa_i)$ is the combination of coefficients in (13c)-(13e) associated with $(\bar{\alpha}_i, \gamma_i)$. Given feasible $(\bar{\alpha}_1, \gamma_1)$ and the solution $\boldsymbol{\omega}_1$, our task is to find a combination $\boldsymbol{\omega}_2 = (\beta_2, \lambda_2, Q_2, \kappa_2)$ such that $(\bar{\alpha}_2, \gamma_2)$ is also feasible in (13c)-(13e). Note that $\bar{\alpha}_2$ and γ_2 are present in different constraints, thus we can discuss their feasibility separately. Firstly we note that the feasibility of constraints (13b) and (13e) will not change when γ is decreased. Secondly, we have $(1-\bar{\alpha}_1)\beta_1 \leq -\kappa_1 - \lambda_1\mu - Q_1(\Sigma + \mu^2) \leq 0$ given a feasible $\bar{\alpha}_1$ in (13c), which implies $\beta_1 \leq 0$. Therefore, we have $(1-\bar{\alpha}_2)\beta_1 \leq (1-\bar{\alpha}_1)\beta_1$ when $\bar{\alpha}_2 \leq \bar{\alpha}_1$. The above discussion implies that we can always ensure the feasibility of $(\bar{\alpha}_2, \gamma_2)$ in (13b)-(13e) by setting the same coefficients $\boldsymbol{w}_2 = \boldsymbol{w}_1$. ■

REFERENCES

[1] S. Parsaeefard and A. Sharafat, "Robust distributed power control in cognitive radio networks," *IEEE Transactions on Mobile Computing*, vol. 12, no. 4, pp. 609–620, April 2013.

[2] S. Huang, X. Liu, and Z. Ding, "Decentralized cognitive radio control based on inference from primary link control information," *IEEE J. Sel. Areas Commun.*, vol. 29, no. 2, pp. 394–406, Feb. 2011.

[3] E. Dall'Anese, S.-J. Kim, G. Giannakis, and S. Pupolin, "Power control for cognitive radio networks under channel uncertainty," *IEEE Trans. Wireless Commun.*, vol. 10, no. 10, pp. 3541–3551, Oct. 2011.

[4] Y. Huang, Q. Li, W.-K. Ma, and S. Zhang, "Robust multicast beamforming for spectrum sharing-based cognitive radios," *IEEE Trans. Signal Process.*, vol. 60, no. 1, pp. 527–533, Jan. 2012.

[5] S. Sun, W. Ni, and Y. Zhu, "Robust power control in cognitive radio networks: A distributed way," in *Proc. IEEE ICC*, June 2011, pp. 1–6.

[6] W. Zhang, Y. Wen, and D. Wu, "Energy-efficient scheduling policy for collaborative execution in mobile cloud computing," in *Proc. IEEE INFOCOM*, Apr. 2013, pp. 190–194.

[7] W. Zhang, Y. Wen, K. Guan, D. Kilper, H. Luo, and D. Wu, "Energy-optimal mobile cloud computing under stochastic wireless channel," *IEEE Trans. Wireless Commun.*, vol. 12, no. 9, pp. 4569–4581, Sep. 2013.

[8] S. Sudevalayam and P. Kulkarni, "Energy harvesting sensor nodes: Survey and implications," *IEEE Commun. Surveys Tuts.*, vol. 13, no. 3, pp. 443–461, Third 2011.

[9] R. Prasad, S. Devasenapathy, V. Rao, and J. Vazifehdan, "Reincarnation in the ambiance: Devices and networks with energy harvesting," *IEEE Commun. Surveys Tuts.*, vol. 16, no. 1, pp. 195–213, First 2014.

[10] Z. Xiang and M. Tao, "Robust beamforming for wireless information and power transmission," *IEEE Wireless Communications Letters*, vol. 1, no. 4, pp. 372–375, August 2012.

[11] D. Wasden, H. Moradi, and B. Farhang-Boroujeny, "Design and implementation of an underlay control channel for cognitive radios," *IEEE J. Sel. Areas Commun.*, vol. 30, no. 10, pp. 1875–1889, Nov. 2012.

[12] M. Gorlatova, A. Wallwater, and G. Zussman, "Networking low-power energy harvesting devices: Measurements and algorithms," in *Proc. IEEE INFOCOM*, Apr. 2011, pp. 1602–1610.

[13] S. Gong, P. Wang, W. Liu, and W. Zhuang, "Performance bounds of energy detection with signal uncertainty in cognitive radio networks," in *Proc. IEEE INFOCOM 2013*, Turin, Italy, Apr. 2013, pp. 2286–2294.

[14] R. M. Gray, *Entropy and Information Theory*. Springer-Verlag New York, Inc., 1990.

[15] C. Huang, R. Zhang, and S. Cui, "Optimal power allocation for outage minimization in fading channels with energy harvesting constraints," *CoRR*, vol. abs/1212.0075, 2012.

[16] S. Zymler, D. Kuhn, and B. Rustem, "Distributionally robust joint chance constraints with second-order moment information," *Mathematical Programming*, vol. 137, no. 1–2, pp. 167–198, 2013.

[17] B. Levy and R. Nikoukhah, "Robust least-squares estimation with a relative entropy constraint," *IEEE Trans. Inform. Theory*, vol. 50, no. 1, pp. 89–104, 2004.

[18] Y. J. A. Zhang, L. Qian, and J. Huang, "Monotonic optimization in communication and networking systems," *Foundations and Trends in Networking*, vol. 7, no. 1, pp. 1–75, 2013.

[19] S. Gong, P. Wang, Y. Liu, and W. Zhuang, "Robust power control with distribution uncertainty in cognitive radio networks," *IEEE J. Sel. Areas Commun.*, vol. 31, no. 11, pp. 2397–2408, Nov. 2013.